2022-04-04

Whole community and functional gene changes of biofilms on marine plastic debris in response to ocean acidification

Kerfahi, D

10.1007/s00248-022-01987-w
Microbial Ecology
Springer Science and Business Media LLC

This paper was published by Springer Nature in *Microbial Ecology* on the 4 April 2022

Kerfahi D., Harvey, B.P., Kim, Y., Yang, Y., Adams, J.M., Hall-Spencer J.M. (2022) Whole community and functional gene changes of biofilms on marine plastic debris in response to ocean acidification. Microbial Ecology. doi.org/10.1007/s00248-022-01987-w 4

Whole community and functional gene changes of biofilms on marine plastic debris in response to ocean acidification

Dorsaf Kerfahi[1,a], Ben P. Harvey[2,a], Hyoki Kim[3], Ying Yang[4], Jonathan M. Adams[*4], Jason M. Hall-Spencer[2,5]

[1]School of Natural Sciences, Department of Biological Sciences, Keimyung University, Daegu 42601, Republic of Korea

[2]Shimoda Marine Research Center, University of Tsukuba, 5-10-1 Shimoda, Shizuoka, Japan

[3]Celemics Inc. 612 Avison Biomedical Research Center, Yonsei Medical Center, Seoul 120-752, Republic of Korea

[4]School of Geographic and Oceanographic Sciences, Nanjing University, Nanjing 210008, China

[5]School of Biological and Marine Sciences, University of Plymouth, Plymouth PL4 8AA, UK

*** Correspondence:**

Jonathan M. Adams: School of Geographic and Oceanographic Sciences, Nanjing University, Nanjing 210008, China.

Phone: (+86)-025-8968-2686

Email: foundinkualalumpur@yahoo.com, jonadams@nju.edu.cn

[a] These authors contributed equally to the work.

Abstract

Plastics are accumulating in the world's oceans, while ocean waters are becoming acidified by increased CO_2. We compared metagenome of biofilms on tethered plastic bottles in subtidal waters off Japan naturally enriched in CO_2, compared to normal ambient CO_2 levels. Extending from an earlier amplicon study of bacteria, we used metagenomics to provide direct insights into changes in the full range of functional genes and the entire taxonomic tree of life in the context of the changing plastisphere. We found changes in taxonomic community composition of all branches of life. This included a large increase in diatom relative abundance across the treatments, but a decrease in diatom diversity. Network complexity amongst families decreased with acidification, showing overall simplification of biofilm integration. With acidification there was decreased prevalence of genes associated with cell-cell interactions and antibiotic resistance, decreased detoxification genes and increased stress tolerance genes. There were few nutrient cycling gene changes, suggesting that the role of plastisphere biofilms in nutrient processes within an acidified ocean may not change greatly. Our results suggest that as ocean CO_2 increases, the plastisphere will undergo broad-ranging changes in both functional and taxonomic composition, especially the ecologically important diatom group, with possible wider implications for ocean ecology.

Keywords: Biofilm; CO_2; Functional genes; Metagenome; Ocean acidification; Plastisphere

1. Introduction

It is estimated that 4.8-12.7 Mt of plastics enter the oceans each year as macroscopic litter and microplastic particles [1, 2]. Larger plastic debris breaks down to produce micro- and nano-plastics [3], but this process is slow, and plastic debris is accumulating in the ocean and impacting marine organisms. Its effects include ingestion and entanglement, which are often fatal [2, 4]. Plastics also provide surfaces for the establishment of microbial biofilms. Biofilms are complex heterogeneous structures consisting of bacteria and other microorganisms within an extracellular matrix, and are found on many artificial and natural surfaces [5, 6]. On rocks and sediment, they play an important role in coastal ecosystems as a major source of primary productivity, and are important nutrient cycling, in supporting food webs and in providing settlement surfaces for establishment of larger sessile organisms [7-11]. It is clear that plastic-associated microbial communities – which are often referred to as the 'plastisphere' [12] – have a distinct taxonomic composition from those found in the surrounding water [12, 13].

Biofilms on plastic can be moved across ocean basins [14], and this may aid the global dispersal of invasive species [15, 16] and pathogens [12]. Marine biofilm communities, including plastic-associated communities, are shaped by local environmental conditions (e.g. temperature, salinity, pH [17, 18] as well as biogeography, season and climate. Better understanding of how environmental factors can shape community composition of the plastisphere will aid understanding of the potential effects these communities can have, for example, on pollutant degradation and biogeochemical cycles and on the rafting of non-native species and pathogens.

Since plastics are both ubiquitous and persistent, it is necessary to consider their interaction with future environments under global change. Little is known of how the plastisphere will be influenced by other major anthropogenic changes to the ocean, such as ocean acidification, which is the alteration of pH and seawater carbonate chemistry due to rising atmospheric CO_2, but it is clear that seawater acidification can affect the community composition and dynamics

of marine ecosystems [19, 20]. Laboratory experiments have increased understanding of responses to increasing concentrations of CO_2 in seawater [21, 22], however it is difficult to scale up from these studies to assess the effects on ocean systems [23]. Natural analogue systems, such as CO_2 seeps, have been used to investigate the ecological consequences of ocean acidification, while retaining natural features such as pH variability and ecological interactions [19, 24]. While previous studies using natural CO_2 seeps have shown that ocean acidification can influence the community composition and diversity of biofilm communities, there has not been any previous work on the biofilm of the plastisphere in this context.

In an earlier paper, we presented preliminary results from our study with exclusively amplicon data of the bacterial community of biofilms grown on PET drinking bottles (which are a conspicuous marine litter problem worldwide) along a natural gradient in seawater carbonate chemistry at carbon dioxide seeps off Japan [25]. We also compared the bacteria of plastics biofilms with free-living and particle-associated bacteria from the same locations. We found substantial changes in the taxonomic composition and functional guild composition of the community [25]. Here, we greatly extend our analysis of these biofilm communities with a study of metagenomes of the same samples. One advantage of metagenomics is that it can give a complete taxonomic picture of biofilm communities, uninfluenced by the limitations of primer ranges and primer bias. Marine biofilms contain a very wide range of taxa, including small animals, fungi archaea and a range of algae, which were not covered in our earlier study of bacteria only. Moreover, using metagenomes it is possible to directly assess the functional gene profile of the biofilm, providing a direct indicator of potential community functions.

Our hypotheses were that: 1) as already shown for the bacterial community exclusively [25], ocean acidification conditions will alter the whole taxonomic composition of the biofilm, and cause changes in the relative abundance of broad groups as well as diversity across archaea, metazoans, fungi and protists. Given that acidification is a novel environmental stress, it is

likely that most taxonomic groups will decline in diversity, as CO_2 concentration increases. We also hypothesized 2) that there would be clear changes in the relative abundance of genes relating to nutrient cycling processes and to the internal stability and integration of the biofilm. Each of these aspects, 1) and 2), could have wide ranging implications for the functional ecology of the global plastisphere, including nutrient cycling, the propensity of marine animals to swallow pieces of plastic due to the biofilm they encountered (based on taste, apparent nutritional content, and appearance), and its rate of biodegradation.

2. Materials and methods

2.1. Study site, experimental set up and sampling

Sampling was carried out on the south coast of Shikine Island, south-east of the Izu Peninsula, Japan (34° 32'N, 139° 20'E). The Izu archipelago is a chain of volcanic islands approximately 150 km south of Tokyo, in the subtropical-temperate zone and influenced by the Kuroshio warm current (Figure S1). At the study site, localized areas with CO_2 bubbling up from the seafloor due to hydrothermal activity cause natural CO_2 enrichment of the shallow coastal water. This provides a range of seawater CO_2 concentrations near the seeps, which match projected ocean acidification conditions. Our experiment was set up to investigate the effect of increasing levels of CO_2 on the microbial biofilm colonizing plastic debris in seawater. The full experimental details were previously described in [25]. Briefly, four locations were chosen along the natural pCO_2 gradient: 'Reference' (mean pCO_2: 410 ± 73), which not influenced by the CO_2 seep; 'medium' (mean pCO_2: 493 ± 158); 'high' (mean pCO_2: 971 ± 258); and 'very high' (mean pCO_2: 1803 ± 1287) (Figure S1). The '971 ± 258 µatm' elevated pCO_2 location represents an end-of-the-21st-century projection for reductions in pH (the RCP 8.5 scenario; IPCC, 2013), and was not confounded by differences in temperature, salinity, dissolved oxygen, total alkalinity, nutrients or depth relative to reference sites used for comparison [19, 20, 26]. The sampling locations and their correspondent carbonate chemistry were previously reported in [20, 25] (Table S1). Clear polyethylene terephthalate (PET) 500 ml bottles were deployed at each location by a scuba diver (six replicates per location, 24 replicates in total). Each PET bottle was floated 15 cm above the seabed, at a depth of 5-6 m Chart Datum, attached by a 5 mm thick string to an anchor bolt in the rock with a small float attached to the top (Figure S2). Each of the PET bottles had been washed with a mild bleach solution and then distilled water before deployment, and handled with sterile gloves. Bottle deployment lasted three weeks from 26th June 2018 until 17th July 2018. Upon sample collection, a 2x5 cm strip of the side of each bottle was collected underwater using sterilized scissors and placed into ziplock bag. On board

RV *Tsukuba II* the PET samples were rinsed with sterile water, placed in a new clean Ziplock bag and stored at -20°C until DNA extraction.

2.2. DNA extraction and PCR amplification

DNA was extracted from the plastic bottle samples by cutting them into small pieces and using a FastDNA SPIN Kit for Soil (MP Biomedicals, LLC, USA) according to the manufacturer's instructions. We performed two replicate DNA extractions per sample, pooling the replicates to obtain sufficient DNA.

2.3. Shotgun metagenomic sequencing and data processing

DNA samples were sequenced for whole metagenome at Celemics (Celemics, Inc., Seoul, Korea) using Illumina HiSeq2000 platform (2 × 150 bp) (Illumina, Inc.). DNA library for metagenome analyses was prepared following the Illumina HiSeq DNA library preparation protocol. The Metagenomics Rapid Annotation (MG-RAST) pipeline was used to annotate the unassembled DNA sequences [27]. The taxonomic and functional profiles were assessed using RefSeq and Subsystems databases, respectively. Sequences having ≥ 5% bp with ≤ 10 phred scores were filtered out before bioinformatics. Raw unassembled reads were annotated in MG-RAST using Hierarchical Classification subsystems with a maximum e value cutoff of 10^{-5}, a minimum percent identity cutoff of 60% and a minimum alignment length cutoff of 15. These profiles were then normalized for differences in sequencing coverage by calculating percent distribution, prior to downstream statistical analysis. The sequences used in this study have been deposited in the MG-RAST server under project ID 91747 (https://www.mg-rast.org/linkin.cgi?project=mgp91747).

2.4. Statistical analysis

Shannon diversity index was calculated from matrices of taxonomic and functional richness, respectively, to estimate the taxonomic and functional alpha-diversity. The deepest assignments of RefSeq taxonomy (species level) and Subsystems function (level 3) were used to calculate the alpha-diversity, as the concept of diversity is based on species level. Variation in the relative abundance of taxonomic groups or functional gene categories among the pH zones was tested using analysis of variance (ANOVA) and Kruskal-Wallis tests for normal and non-normal data, respectively in R software package 2.14.2. Furthermore, parametric (Tukey's HSD test) or nonparametric (pairwise Wilcox test) post hoc tests were used following significant results from the ANOVA or Kruskal–Wallis tests, respectively.

To assess whether plastic microbial community composition clustered according to different pH levels, we performed a non-metric multidimensional scaling (nMDS) plot of taxonomy (ReSeq taxonomic profile at class level) and function (Subsystems at function level 3) using the metaMDS function in the Vegan package of R. This used the Bray–Curtis distance matrix to assess patterns in species composition. A permutational multivariate analysis of variance (PERMANOVA) was performed with 999 permutations using the Adonis function in Vegan R package [28].

To understand the co-occurrence relationships between taxonomic families, we performed network analysis. The network analysis (based on statistically significant tests of correlation) provides a tool to understand the ecosystem functioning and offers a more intricate measure of the interactions between different taxa [29, 30]. The connectivity between members of microbial communities can also indicate the robustness of ecosystem functioning. All possible Spearman's rank correlation coefficients were calculated and only correlations with $r > 0.9$ and $p < 0.01$ were selected to reduce the network complexity. The network topology was described based on set of measures, average clustering coefficients, average path length, and modularity. The interactive platform Gephi was used to explore and visualize the structure of the network. Modularity describes a network that could be naturally divided into communities or modules.

The network modules were generated using rapid greedy modularity optimization [31]. The ecological role of each node in the microbial network can be reflected by among module connectivity (Pi) and within-module connectivity (Zi). The connectivity within (Zi) or between (Pi) modules of molecular ecological networks reflects the topological role of each node, Zi reflects how close a node is connected to other nodes within its own module, and Pi describes how close a node contacts with different modules. The topological roles of different nodes can be categorized into four types: peripherals ($Zi \leq 2.5$, $Pi \leq 0.62$), connectors ($Zi \leq 2.5$, $Pi > 0.62$), module hubs ($Zi > 2.5$, $Pi \leq 0.62$) and network hubs ($Zi > 2.5$, $Pi > 0.62$) [32, 33]. Generally, connectors, module hubs and network hubs are considered as putative keystone species of ecological network [31].

192 ## 3. Results

193 ### 3.1. Water physico-chemical parameters of the sites compared

194 In Table S1 we have added water chemistry parameters that were presented in our earlier study
195 on bacteria [25]. These show that water chemistry was identical except for pH, dissolved CO_2,
196 calcium and aragonite concentration –explicable in terms of CO_2 enrichment [24]. Slight
197 differences in water temperature were observed – attributable to slightly different sampling
198 times during the tidal cycle.

199

200 ### 3.2. Dominant microbial taxa in shotgun metagenomics sequences

201 A total of 104 million good quality filtered reads were obtained from 24 samples through
202 shotgun metagenomic sequencing (Table S2). Approximately 32–47% of the total metagenomic
203 sequences were annotated to a protein of known function using e value $<1 \times 10^{-5}$ and 15-bp
204 minimum alignment length. Bacterial sequences were most dominant in the metagenomic
205 sequence data (90.3% of all sequences) followed by Eukaryotes (9.3%) and Archaea (0.4%),
206 with less than 0.1% for viruses (Figure 1A). Diatoms accounted for an average abundance of
207 4.3% of total sequences. Their relative abundance increased with increasing CO_2 concentrations
208 (Figure 1B). Proteobacteria was the most abundant phylum across all plastic samples (57.6%
209 on average), followed by Bacteroidetes (16%), Cyanobacteria (6.8%), Bacillariophyta (4.4%),
210 and to a lesser degree Actinobacteria (2.6%), Firmicutes (2%), with the other phyla (including
211 Planctomycetes, Verrucomicrobia, and Chloroflexi) each comprising of less than 2% of the
212 abundance. The relative abundance of almost all detected phyla on the plastic samples differed
213 between the different CO_2 concentration levels, apart from Proteobacteria ($F_{3,20} = 1.36$,
214 $p = 0.284$) and Cyanobacteria ($F_{3,20} = 1.48$, $p = 0.249$) which were not significantly affected.
215 The relative abundance of Bacteroidetes ($F_{3,20} = 13.76$, $p < 0.001$), Firmicutes ($F_{3,20} = 6.14$,
216 $p = 0.003$), Planctomycetes ($F_{3,20} = 13.78$, $p < 0.001$), Verrucomicrobia ($F_{3,20} = 10.93$,
217 $p < 0.001$) and Chloroflexi ($F_{3,20} = 4.11$, $p = 0.019$) decreased with increasing CO_2

concentration. However Bacillariophyta (diatoms) ($\chi^2_3 = 17.19$, $p < 0.001$) and Actinobacteris ($\chi^2_3 = 9.48$, $p = 0.023$) increased at higher CO_2 sites (Figure 2).

At the family level, most common microbial families significantly differed with increasing pCO_2, except for a few families such as Nostocacea, Bradyrhizobia and Myxcoccacea which did not significantly differ. Flavobacteriacea, Cytophagacea, Hyphomonadacea, Planctomycetacea, Sphingobacteriacea, Solibacteriacea, and Verrucomicrobia decreased in abundance at higher CO_2 sites. In contrast, Rhodobacteriacea, Phaeodactlylacea Rhizobiacea, Erythrobacteriacea, Phyllobacteriacea and Methylophilacea increased at acidified sites. Some other families including Hyphomonadacea, Pseudomonadacea, Alteromonadacea and Vibrionacea increased at medium CO_2 then their relative abundance decreased at higher CO_2 sites (Figure S3, Table S3).

3.3. Key gene group relative abundances

The shotgun metagenomic sequences were grouped into 28 functional gene categories at subsystem level 1. Of these, 18 categories significantly differed between sites along the CO_2 gradient (Table 1). The gene categories associated with stress response ($F_{3,20} = 12.9$, $p < 0.001$), phages and prophages ($\chi^2_3 = 14.55$, $p = 0.002$), and aromatic compounds' metabolism ($F_{3,20} = 6.2$, $p = 0.003$) had higher relative abundance at higher CO_2 sites. However, genes related to secondary metabolism ($F_{3,20} = 7.17$, $p = 0.001$), iron acquisition and metabolism ($F_{3,20} = 51.99$, $p < 0.001$), and virulence diseases and defense ($F_{3,20} = 8.36$, $p < 0.001$) decreased in abundance with increased CO_2. Genes associated with nitrogen cycle increased at medium CO_2 then decreased at very high CO_2 ($F_{3,20} = 8.54$, $p < 0.001$) (Table 1; Figure 3).

The analysis of the microbial gene functions at lower functional level (levels 2 and 3) showed that overall genes related to heat shock ($F_{3,20} = 5.53$, $p = 0.006$), oxidative stress ($F_{3,20} = 2.93$, $p = 0.05$), osmotic stress ($F_{3,20} = 14.46$, $p < 0.001$), and detoxification ($F_{3,20} = 12.41$, $p < 0.001$)

increased with acidification (at lower pH sites); while genes associated with resistance to antibiotics and toxic compounds ($\chi^2_3 = 11.51$, $p = 0.009$), invasion and interaction resistance ($F_{3,20} = 8.14$, $p < 0.001$), nitrate and nitrite ammonification ($\chi^2_3 = 7.72$, $p = 0.05$), and nitrogen fixation ($\chi^2_3 = 7.71$, $p = 0.05$) decreased at acidified sites (Figure 4). Functional genes related to bacteria showed the same pattern as the above overall functions including all taxonomic groups, except for few functional genes (example bacterial respiration ($F_{3,20} = 6.05$, $p = 0.004$) increased with acidification, the overall respiration ($F_{3,20} = 0.56$, $p = 0.64$) did not statistically differ between different CO_2 levels (Table S4).

3.4. Taxonomic and functional diversity and community structure

Our results showed that overall taxonomic diversity based on Shannon index calculated at RefSeq species level differed between plastic samples at different CO_2 level ($\chi^2_3 = 11.81$, $p = 0.008$), with very high CO_2 site harbored the lowest microbial diversity (Figure 5A). Taxonomic microbial diversity of plastic microbial subgroups (Figure S5) showed a variation among different CO_2 levels except for bacteria ($\chi^2_3 = 5.3$, $p = 0.15$). Both eukaryal ($\chi^2_3 = 16.12$, $p = 0.001$) and fungal ($\chi^2_3 = 15.86$, $p = 0.001$) taxonomic diversities decreased at acidified sites, with lowest diversity observed at very high CO_2 concentration (Figure S4). Despite the increase in the relative abundance of diatoms, their diversity decreased at higher CO_2 ($\chi^2_3 = 19.36$, $p = 0.002$) (Figure S4). Archaeal taxonomic diversity increased at higher CO_2 sites ($\chi^2_3 = 12.55$, $p = 0.005$) (Figure S4). Functional diversity using Shannon index and calculated at Subsystems function level 3 showed the opposite pattern as the overall taxonomic diversity ($F_{3,20} = 4.01$, $p = 0.021$), with lowest functional diversity found at the lowest CO_2 sites (Figure 5B). Microbial community composition on plastics revealed a significant difference between sites. Cluster analysis of Bray-Curtis distance based on both taxonomy at class level

(Global R = 0.646, $p = 0.001$) and function level 3 (Global R = 0.339, $p = 0.002$) showed that microbial community composition was distinct at each CO_2 level (Figure 6).

3.5. Connectivity analysis and keystone families

Correlation-based network analysis was conducted to study the connectedness of the system [30], based on examining microbial families' connectivity via network analyses (Figure 7). The microbial taxa presenting the highest number of correlations with other taxonomic groups are shown in Table 2. These families include Acidobacteriaceae, Pseudomonadaceae, Thermomonosporaceae, Pelobacteraceae, and Nitrospiraceae. There were 362, 391, 327 and 229 nodes in reference CO_2, medium CO_2, high CO_2, and very high CO_2 networks, respectively, Table 2). The more acidified sites (high and very high CO_2) had a lower number of nodes and links and increased modularity, with very high CO_2 site having the fewest nodes and edges compared with other sites (Figure 7).

Taxonomic families take different topological roles in the ecological networks (Figure 8). There were 148 nodes classified as module hubs and six nodes for connectors in the network. Most of the connectors in the network originated from the families Chabertiidae, Piptocephalidaceae, and Hypogastruridae. The module hubs belonged to the bacterial families Acetobacteraceae, Acidobacteriaceae, Halobacteroidaceae, Gemmatimonadaceae, and Clostridiaceae (Table S5). The number of module hubs was far greater than that of connectors, which indicated that the ecological network modules were scattered and the connection between modules was weak.

4. Discussion

In this study, metagenome analysis was utilized to provide a broader and more complete picture of how the taxonomic composition and functional gene composition of the biofilm on plastic responded to ocean acidification conditions. Our metagenome analysis revealed the very diverse taxonomic composition of the plastic biofilm. At every seawater pH/CO_2 level we studied, it contained a very diverse community. All major categories of life, including bacteria, archaea, viruses, and major groups of eukaryotes (including diatoms, fungi, protists, and metazoans) were present in the plastisphere biofilm. To our knowledge, this is the first study which has used a metagenome approach to consider how the plastisphere is affected by ocean acidification.

As we had hypothesized, comparison between the treatments revealed substantial differences in broad level taxonomic composition of the biofilm between the different CO_2 levels. The most striking difference (Figure 1B) was in the relative abundance of diatoms in the biofilm. In the two higher CO_2 treatments, representing future acidified ocean scenarios, there was a large increase in relative abundance of diatoms and of eukaryotes in general, while the relative abundance of bacteria decreased. Also as hypothesized, taxonomic diversity differed between treatments, with a decline in family level diversity of bacteria, fungi, metazoans, protista and diatoms. However, archaea showed an increase in family level diversity. While it is difficult to assess the potential impact of diversity differences, the differences in relative abundance could have implications for the ecology of ocean plastics in a future world with acidified oceans. Diatoms play a major role in ocean systems worldwide, including biofilms, in which they secrete a polysaccharide layer that forms part of the integral structure of the biofilm. If the changing composition of this layer alters the palatability of the plastics to marine animals, it may affect their tendency to swallow the plastics. Through screening out of UV light by 'sunscreen' compounds in the diatom cells and their matrix [34, 35], increases in diatom relative

312 abundance may affect the ability of sunlight to degrade the plastic over time. Such changes in
313 relative abundance might also affect the physical durability of the biofilm layer, and its tendency
314 to degrade under UV light or through chemical alteration.
315 Overall, across the different CO_2 treatments there was a stability in the relative abundance of
316 major gene functions present in the metagenomes. There were only a few clear changes in the
317 relative abundance of functional genes that could potentially affect nutrient cycling by these
318 biofilms. Genes involved in the processes of nitrogen fixation, ammonification, and
319 denitrification, for instance, did not significantly differ in relative abundance between reference
320 and higher seawater CO_2 treatments (Figure 4, Table 1). This suggests that the role of plastic
321 biofilms as potential bioreactors in the ocean nutrient cycle (e.g. in promoting nitrogen fixation,
322 or ammonia oxidation) will not change greatly.
323 However, there were changes in relative abundance of genes related to nutrient uptake of iron.
324 With increasing acidification, there was a decrease in relative abundance of genes relating to
325 iron acquisition and metabolism (e.g. genes associated with iron acquisition in *Vibrio*,
326 siderophores, etc.) (Table S4). Conversely, genes relating to phosphorous uptake and processing
327 (e.g. phosphate metabolism) did not show any change. Both Fe and P are important limiting
328 nutrients in ocean systems and the direction of change in Fe uptake genes implies that they
329 could become less important in terms of the influence of plastic biofilms on nutrient cycles in
330 an acidified global ocean – however there is no sign that P uptake will differ.
331 Decreased prevalence of genes associated with cell-cell interactions (e.g. regulation and cell
332 signalling genes, genes related to cell wall and capsule) suggested weaker biofilm integration
333 and resilience. There was an increase in heat shock, oxidative and osmotic stress genes (e.g.
334 osmoregulation genes, genes related to heat inducible transcription repressor HrcA, etc.) with
335 acidification, suggesting more intense environmental stress and decreased resilience of the
336 biofilm community (Table S4), a factor which may be of additional significance in a warmer
337 future ocean under global warming. Increasing acidification was associated with an increase in

338 relative abundance of genes associated with detoxification and aromatic compound breakdown
339 (such as genes related to glutathione dependent pathway of formaldehyde detoxification, genes
340 related to the uptake of selenate and selenite, genes related to the metabolism of central aromatic
341 intermediates, genes related to peripheral pathways for catabolism of aromatic compounds, etc.)
342 suggesting increased ability to degrade xenobiotic pollutants, a potential plus side to ocean
343 acidification if plastics biofilms can act as bioreactors 'cleaning' the ocean water. There has
344 been concern that plastic biofilms could act to transport antibiotic resistant pathogens or
345 resistance genes . Our metagenome samples suggested that antibiotic resistance genes (Figure
346 4) will become relatively less abundant under ocean acidification.
347 Our network analyses (Figure 7) showed that the connectivity amongst microbial families
348 decreased with acidification, with higher CO_2 sites having the least number of correlations
349 compared with reference and medium CO_2 levels. Our findings mirror our expectation that an
350 undisturbed system should have greater network complexity due to its stable and predictable
351 interactions [36]. However, our findings contrast with those of another study [37], where
352 climate warming enhanced the complexity of microbial connectivity and strengthened the
353 network structure, leading to a higher community stability as the network stability significantly
354 correlated with network complexity. However, our study – while projecting the future – did not
355 deal with climate change and only with changes in carbonate chemistry of the oceans. It would
356 be interesting to combine a warming effect with an ocean pH change, to reflect future changes
357 more realistically.
358 The initial snapshot provided by this small-scale experiment provides a range of intriguing clues
359 to what may happen to biofilm plastics over future decades and centuries as the global ocean
360 acidifies. It appears that plastisphere will undergo significant changes with changes in
361 taxonomic composition towards a greater role for diatoms, and changes in xenobiotic
362 degradation and nutrient cycling that could have wider implications for ocean ecology. There
363 is now a need for further work, involving more studies – both in a wider range of field sites and

laboratory mesocosms. Our experiment dealt with only the first weeks of biotic succession on a plastic surface, while plastic may potentially circulate in the surface waters for years or even decades before it degrades into smaller fragments to form microplastics [38, 39]. Thus, there is a need to study longer time series of ecological succession on plastic biofilms under ocean acidification conditions: these could be more relevant for understanding the changing effect of the plastisphere on ocean nutrient cycling and pollutant breakdown .

5. Conclusions

In conclusion, a metagenomic approach revealed a diverse biota spanning several kingdoms of life existing in plastics biofilms, across different levels of ocean acidification. The most striking change with acidification was in the relative abundance of diatoms, a group of major importance in ocean ecology. The network structure of the whole taxonomic community also showed decreased connectivity between the taxonomic families with increasing pCO_2. Overall, the abundance of gene functions involved in nutrient cycling remained fairly stable, except for a change in Fe uptake genes, but stress-related genes increased in more acidified conditions, suggesting physiological stress. Taxonomic simplification, decreased network integration and increased stress responses may decrease biofilm resilience, and together with the increased role of diatoms these changes deserve further investigation from the point of view of ocean ecology.

Acknowledgement

We thank the technical staff at the Shimoda Marine Research Center, University of Tsukuba for their field assistance.

Declarations

Funding

This work has received funding from Japan Society for the Promotion of Science (JSPS) KAKENHI (grant number 17K17622), and the Ministry of the Environment, Government of Japan (Suishinhi: 4RF-1701), and the Bisa Research grant of Keimyung University in 2020, Republic of Korea.

Conflicts of interest/Competing interests

The authors declare that they have no known competing financial interests or personal relationships that could have appeared to influence the work reported in this paper.

Data availability

The sequences used in this study have been deposited in the MG-RAST server under project ID 91747 (https://www.mg-rast.org/linkin.cgi?project=mgp91747).

Code availability

Not applicable.

Authors' contributions

Dorsaf Kerfahi: Conceptualization, Investigation, Methodology, Analysis, Writing – original draft. Ben P. Harvey: Conceptualization, Resources, Methodology, Investigation, Writing – Review and editing. Hyoki Kim: Investigation, Resources. Ying Yang: Investigation, Analysis. Jonathan M. Adams: Conceptualization, Methodology, Resources, Writing - Review and editing. Jason M. Hall-Spencer: Conceptualization, Methodology, Investigation, Supervision, Writing - Review and editing.

Ethics approval

Not applicable.

Consent to participate

Not applicable.

Consent for publication

The authors give their consent for publication, if manuscript is accepted.

References

1. Geyer R, Jambeck JR, Law KL (2017) Production, use, and fate of all plastics ever made. Sci Adv 3: e1700782.
2. Worm B, Lotze HK, Jubinville I, Wilcox C, Jambeck J (2017) Plastic as a persistent marine pollutant. Ann Rev Environ Res 42.
3. Galloway TS, Lewis CN (2016) Marine microplastics spell big problems for future generations. Proc Natl Acad Sci 113: 2331-2333.
4. Thompson RC, Moore CJ, Vom Saal FS, Swan SH (2009) Plastics, the environment and human health: current consensus and future trends. Philos Trans R Soc B: Biol Sci 364: 2153-2166.
5. Lock M (1993) Attached microbial communities in streams. Aquatic microbiology: an ecological approach: 113-138.
6. Krumbein WE, Brehm U, Gerdes G, Gorbushina AA, Levit G, Palinska KA (2003) Biofilm, biodictyon, biomat microbialites, oolites, stromatolites geophysiology, global mechanism, parahistology Fossil and recent biofilms. Springer, pp. 1-27
7. Hawkins SJ, John DM, Price JH (1992) Plant-Animal interactions in the marine benthos. Syst Assoc.
8. Thompson R, Norton T, Hawkins S (2004) Physical stress and biological control regulate the producer–consumer balance in intertidal biofilms. Ecology 85: 1372-1382.
9. Dang H, Lovell CR (2016) Microbial surface colonization and biofilm development in marine environments. Microbiol Mole Biol Rev 80: 91-138.
10. Lau SC, Thiyagarajan V, Cheung SC, Qian P-Y (2005) Roles of bacterial community composition in biofilms as a mediator for larval settlement of three marine invertebrates. Aquat Microb Ecol 38: 41-51.
11. Qian P-Y, Lau SC, Dahms H-U, Dobretsov S, Harder T (2007) Marine biofilms as mediators of colonization by marine macroorganisms: implications for antifouling and aquaculture. Mar Biotechnol 9: 399-410.
12. Zettler ER, Mincer TJ, Amaral-Zettler LA (2013) Life in the "plastisphere": microbial communities on plastic marine debris. Environ Sci Technol 47: 7137-7146.
13. McCormick A, Hoellein TJ, Mason SA, Schluep J, Kelly JJ (2014) Microplastic is an abundant and distinct microbial habitat in an urban river. Environ Sci Technol 48: 11863-11871.
14. Jokiel PL (1990) Long-distance dispersal by rafting: reemergence of an old hypothesis. Endeavour 14: 66-73.
15. Barnes DK (2002) Invasions by marine life on plastic debris. Nature 416: 808-809.
16. Rochman CM, Browne MA, Underwood AJ, Van Franeker JA, Thompson RC, Amaral-Zettler LA (2016) The ecological impacts of marine debris: unraveling the demonstrated evidence from what is perceived. Ecology 97: 302-312.
17. Toyofuku M, Inaba T, Kiyokawa T, Obana N, Yawata Y, Nomura N (2016) Environmental factors that shape biofilm formation. Biosci Biotechnol Biochem 80: 7-12.
18. Oberbeckmann S, Kreikemeyer B, Labrenz M (2018) Environmental factors support the formation of specific bacterial assemblages on microplastics. Front Microbiol 8: 2709.
19. Agostini S, Harvey BP, Wada S, Kon K, Milazzo M, Inaba K, Hall-Spencer JM (2018) Ocean acidification drives community shifts towards simplified non-calcified habitats in a subtropical− temperate transition zone. Sci Rep 8: 11354.
20. Harvey BP, Agostini S, Kon K, Wada S, Hall-Spencer JM (2019) Diatoms dominate and alter marine food-webs when CO_2 rises. Diversity 11: 242.
21. Dupont S, Pörtner H (2013) Get ready for ocean acidification. Nature 498: 429-429.

22. Riebesell U, Gattuso J-P (2014) Lessons learned from ocean acidification research. Nat Clim Change 5: 12. doi: 10.1038/nclimate2456
23. Hall-Spencer JM, Harvey BP (2019) Ocean acidification impacts on coastal ecosystem services due to habitat degradation. Emerg Top Life Sci 3: 197-206.
24. Hall-Spencer JM, Rodolfo-Metalpa R, Martin S, Ransome E, Fine M, Turner SM, Rowley SJ, Tedesco D, Buia M-C (2008) Volcanic carbon dioxide vents show ecosystem effects of ocean acidification. Nature 454: 96.
25. Harvey BP, Kerfahi D, Jung Y, Shin J-H, Adams JM, Hall-Spencer JM (2020) Ocean acidification alters bacterial communities on marine plastic debris. Mar Pollut Bull 161: 111749.
26. Agostini S, Wada S, Kon K, Omori A, Kohtsuka H, Fujimura H, Tsuchiya Y, Sato T, Shinagawa H, Yamada Y (2015) Geochemistry of two shallow CO_2 seeps in Shikine Island (Japan) and their potential for ocean acidification research. Reg Stud Mar Sci 2: 45-53.
27. Meyer F, Paarmann D, D'Souza M, Olson R, Glass EM, Kubal M, Paczian T, Rodriguez A, Stevens R, Wilke A (2008) The metagenomics RAST server–a public resource for the automatic phylogenetic and functional analysis of metagenomes. BMC bioinformatics 9: 386.
28. Oksanen J, Kindt R, Legendre P, O'Hara B, Stevens MHH, Oksanen MJ, Suggests M (2007) The vegan package. Community ecology package 10: 631-637.
29. Barberán A, Bates ST, Casamayor EO, Fierer N (2012) Using network analysis to explore co-occurrence patterns in soil microbial communities. The ISME J 6: 343.
30. Faust K, Raes J (2012) Microbial interactions: from networks to models. Nat Rev Microbiol 10: 538-550.
31. Olesen JM, Bascompte J, Dupont YL, Jordano P (2006) The smallest of all worlds: pollination networks. J Theor Biol 240: 270-276.
32. Deng Y, Jiang Y-H, Yang Y, He Z, Luo F, Zhou J (2012) Molecular ecological network analyses. BMC bioinformatics 13: 1-20.
33. Cong J, Yang Y, Liu X, Lu H, Liu X, Zhou J, Li D, Yin H, Ding J, Zhang Y (2015) Analyses of soil microbial community compositions and functional genes reveal potential consequences of natural forest succession. Sci Rep 5: 1-11.
34. Cooksey K, Wigglesworth-Cooksey B (1995) Adhesion of bacteria and diatoms to surfaces in the sea: a review. Aquat Microb Ecol 9: 87-96.
35. Eich A, Mildenberger T, Laforsch C, Weber M (2015) Biofilm and diatom succession on polyethylene (PE) and biodegradable plastic bags in two marine habitats: early signs of degradation in the pelagic and benthic zone? PloS one 10: e0137201.
36. Wagg C, Bender SF, Widmer F, van der Heijden MGA (2014) Soil biodiversity and soil community composition determine ecosystem multifunctionality. Proc Natl Acad Sci 111: 5266-5270. doi: 10.1073/pnas.1320054111
37. Yuan MM, Guo X, Wu L, Zhang Y, Xiao N, Ning D, Shi Z, Zhou X, Wu L, Yang Y (2021) Climate warming enhances microbial network complexity and stability. Nat Clim Change 11: 343-348.
38. Shah AA, Hasan F, Hameed A, Ahmed S (2008) Biological degradation of plastics: a comprehensive review. Biotechnol Adv 26: 246-265.
39. Fotopoulou KN, Karapanagioti HK (2017) Degradation of various plastics in the environment Hazardous Chemicals Associated with Plastics in the Marine Environment. Springer, pp. 71-92

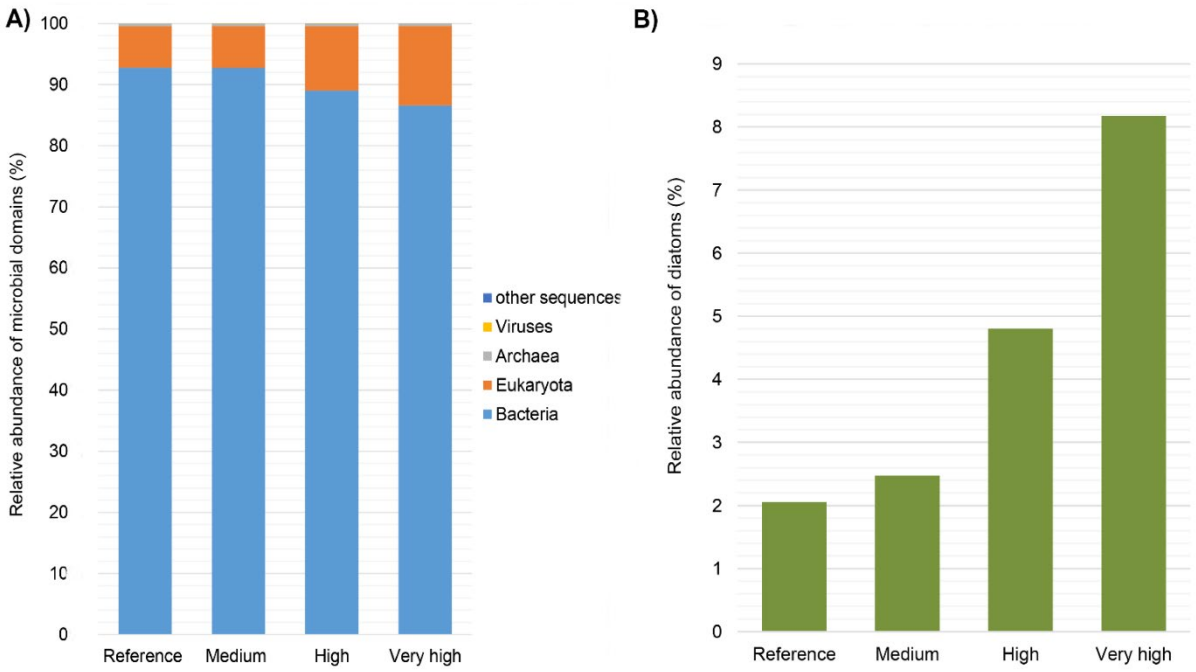

510

511 **Figure 1**. Relative abundance of reads of **(A)** microbial taxa at the domain level and **(B)** diatoms

512 on plastic samples at different CO_2 levels.

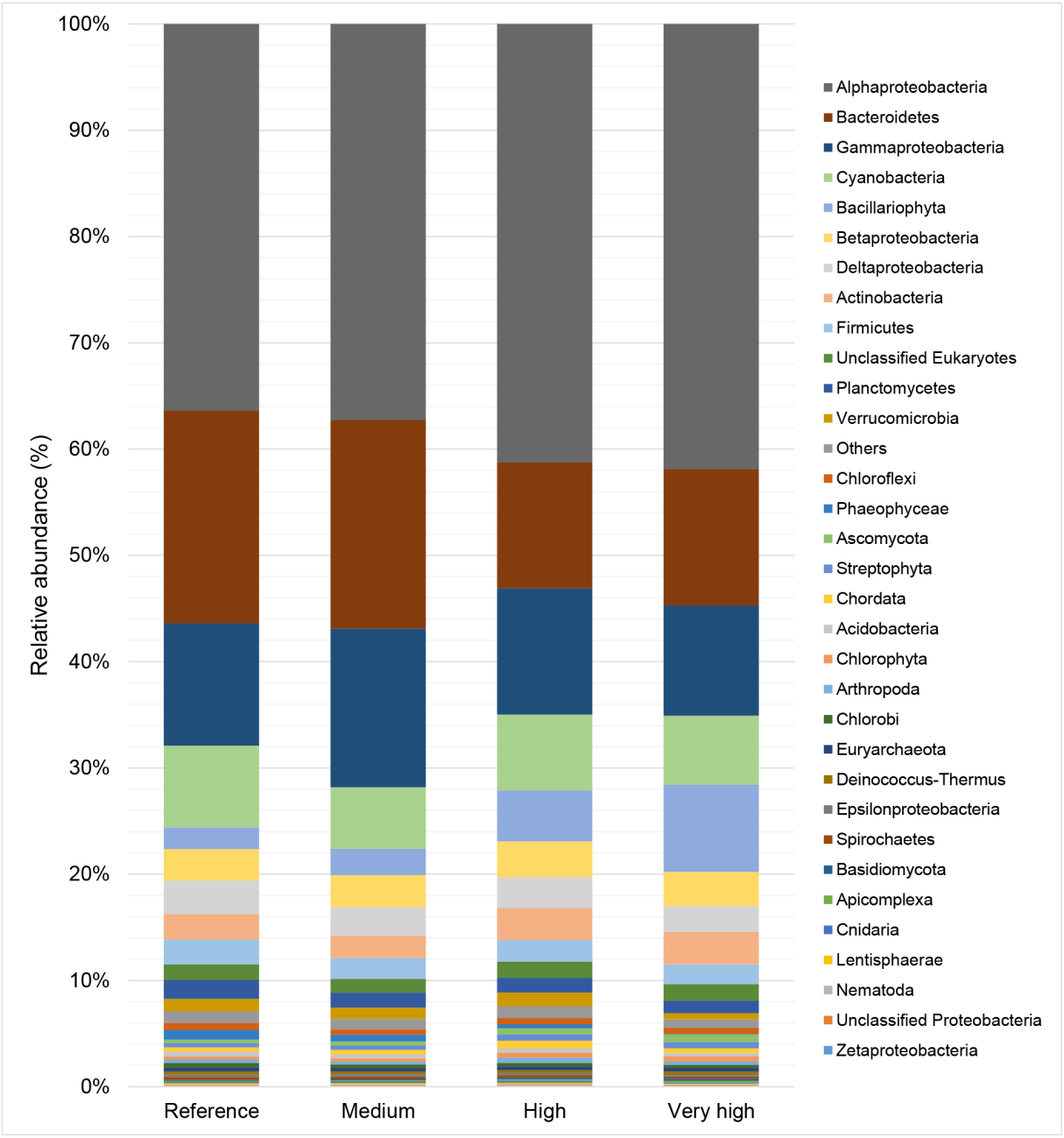

Figure 2. Relative abundance of detected microbial communities across different CO_2 levels at the phylum level.

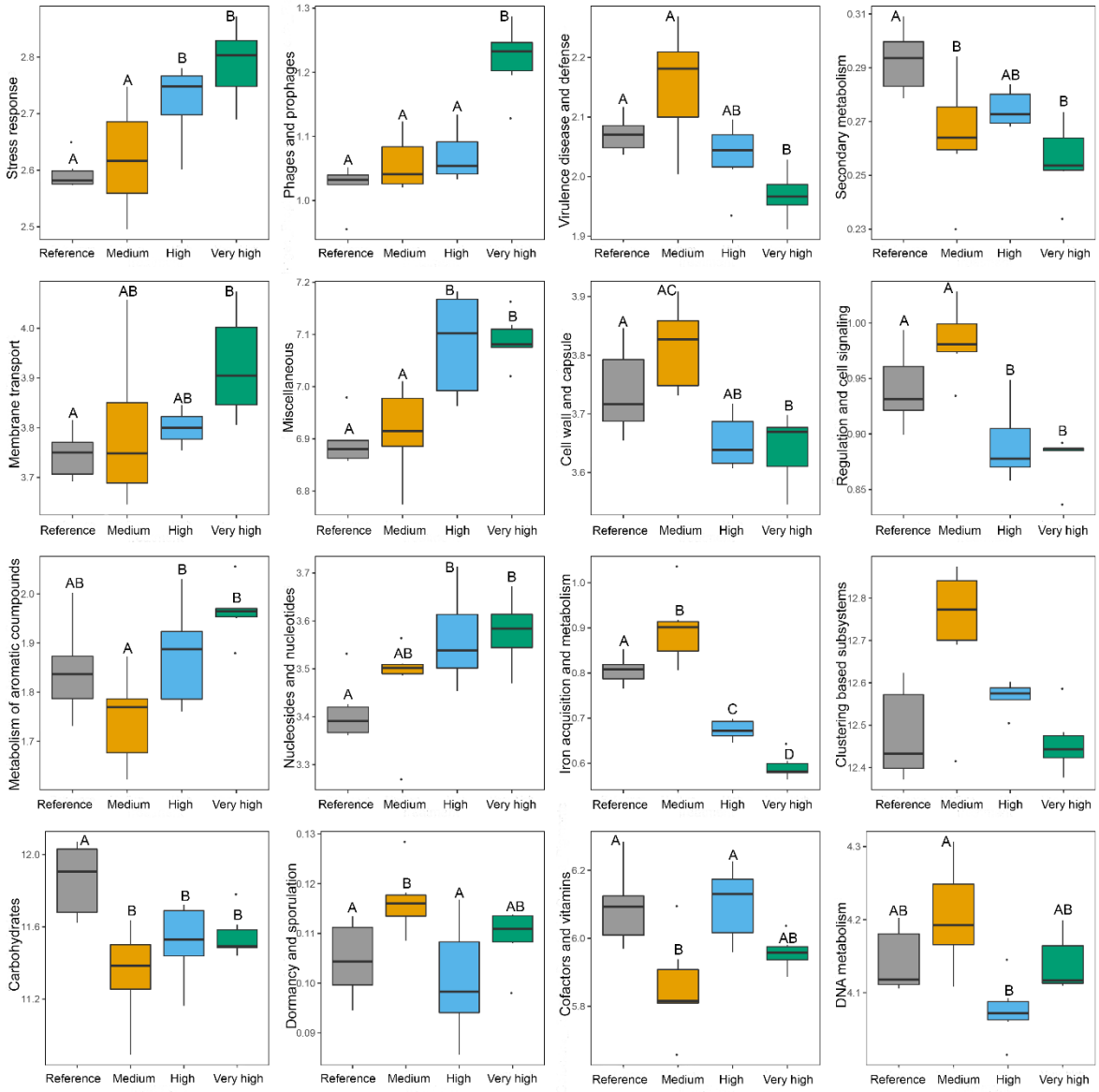

516

517 **Figure 3.** Variation of microbial functions at Subsystems function level 1 on plastic samples at

518 different CO_2 levels. Pairwise comparisons were made using Benjamini–Hochberg method, and

519 different letters denote significant differences ($p < 0.05$).

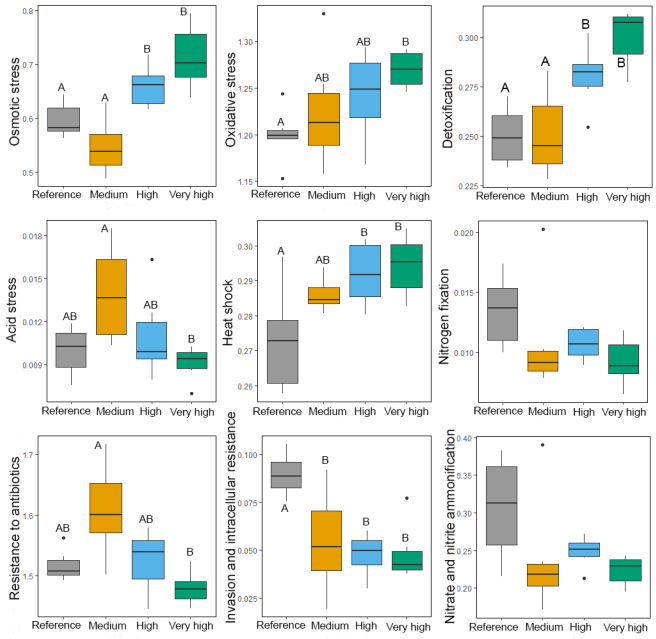

520

521 **Figure 4.** Relative abundance of genes related to stress, virulence and nitrogen at different CO_2
522 levels. Pairwise comparisons were made using Benjamini–Hochberg method, and different
523 letters denote significant differences ($p < 0.05$).

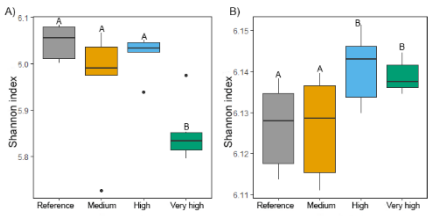

524

525 **Figure 5. (A)** Taxonomic diversity at species level and **(B)** functional diversity at function level
526 3 of plastic microbial communities at different CO_2 levels based on Shannon index. Pairwise
527 comparisons were made using Benjamini–Hochberg method, and different letters denote
528 significant differences ($p < 0.05$).

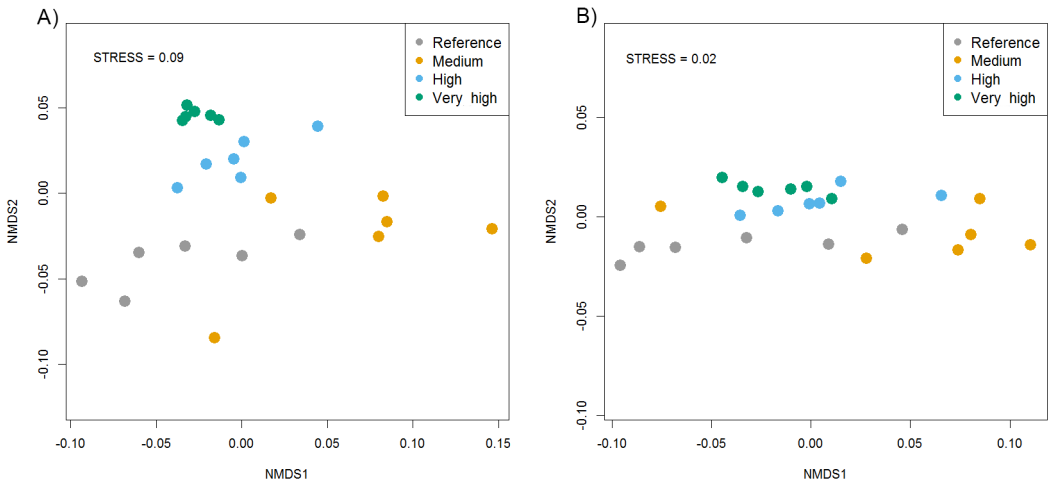

529

530 **Figure 6.** NMDS ordination based on Bray-Curtis distance of microbial community
531 composition of **(A)** RefSeq taxonomic profile at class level, and **(B)** Subsystem functional level
532 3 of shotgun metagenomic sequences from samples of different CO_2 levels.

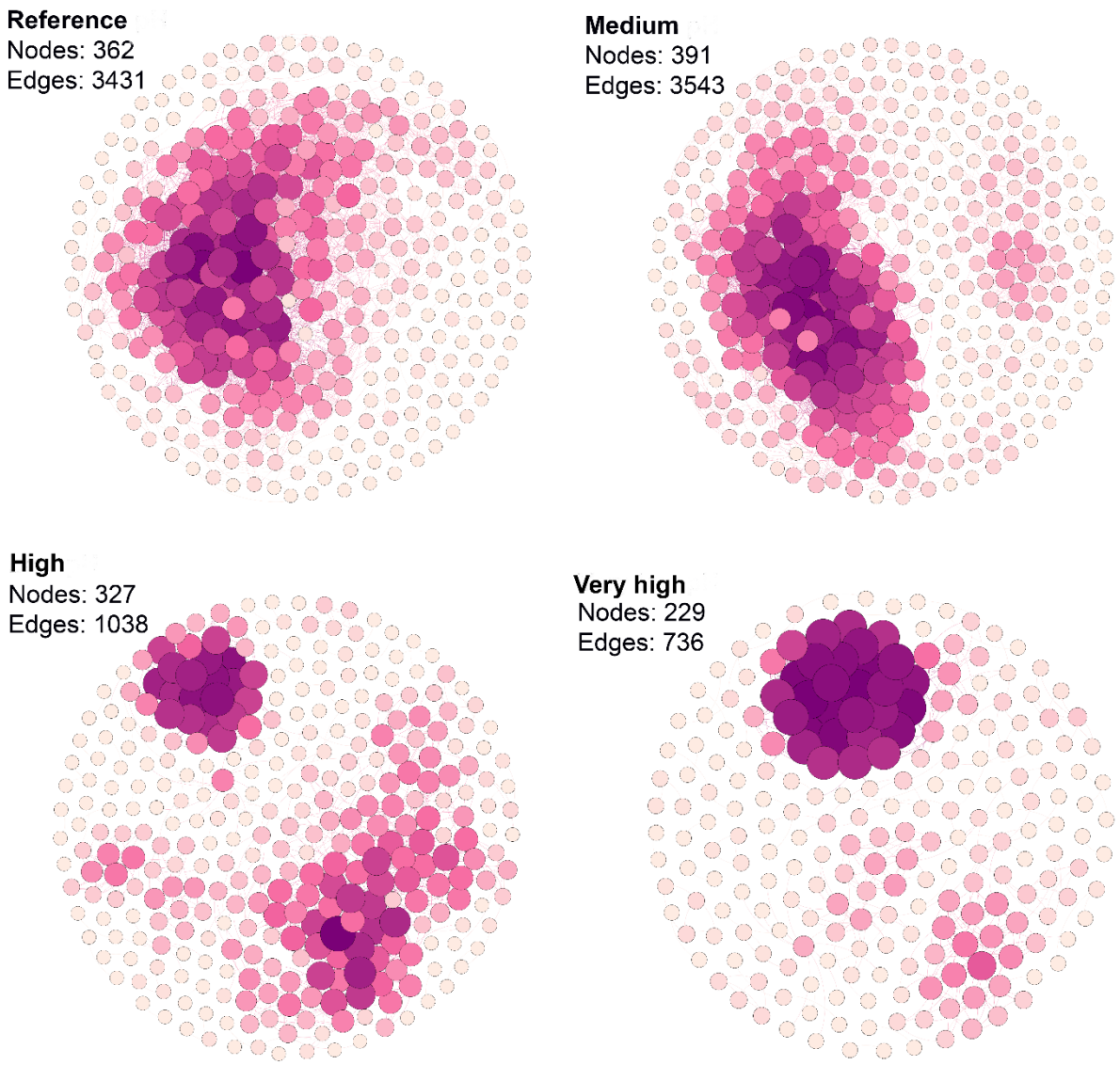

533

534 **Figure 7.** Network interactions of microbial communities on plastics at different CO_2 levels,
535 based on correlation analysis of the RefSeq taxonomic profile at the family level. Each edge
536 stands for strong (Spearman's correlation coefficient $r > 0.9$) and significant ($p < 0.01$)
537 correlations. The size of each node is proportional to the number of connections.

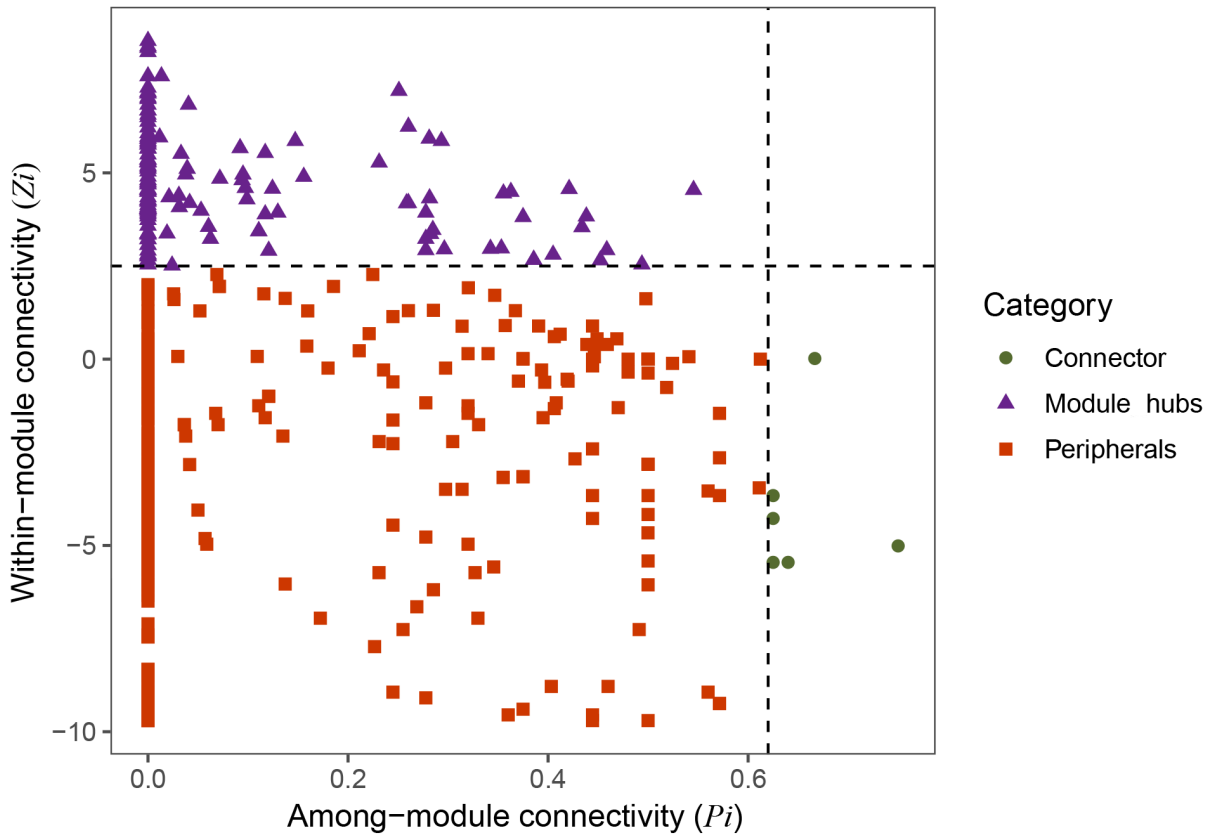

538

539 **Figure 8.** Z-P plot showing the distribution of families based on their topological roles. Each

540 symbol represents a family.

541 **Table 1.** Relative abundance of functional gene categories at subsystem level 1 (Subsystem

542 database) in plastic samples at different CO_2 levels†.

Table 1. Relative abundance of functional gene categories at subsystem level 1 (Subsystem database) in pla
CO_2 levels†.

Functional gene categories	Reference	Medium	High
Clustering based subsystems	12.48±0.118	12.73±0.16	12.57±0.03
Carbohydrates	11.86±0.2a	11.34±0.26b	11.52±0.21b
Miscellaneous	6.9±0.04a,b	6.91±0.08a,b	7.08±0.1c
Cofactors, vitamins, prosthetic groups, pigments	6.09±0.11a	5.85±0.14b	6.1±0.1a
DNA metabolism	4.14±0.04a,b	4.2±0.07a	4.07±0.04b
Membrane transport	3.74±0.04a	3.8±0.15a,b	3.8±0.03a,b
Cell wall and capsule	3.74±0.07a	3.81±0.07a,c	3.65±0.04a,b
Nucleosides and nucleotides	3.41±0.06a	3.47±0.1a,b	3.56±0.09b
Stress response	2.6±0.02a	2.62±0.09a	2.72±0.06b
Virulence, disease and defense	2.07±0.02a	2.15±0.09a	2.03±0.05a,b
Metabolism of aromatic compounds	1.84±0.09a,b	1.74±0.09a	1.87±0.1b
Phages, prophages, transposable elements, plasmids	1.02±0.03a	1.05±0.04a	1.06±0.04a
Sulfur metabolism	0.88±0.02a	0.94±0.05a	1.03±0.03b
Regulation and cell signaling	0.94±0.03a	0.98±0.03a	0.9±0.03b
Iron acquisition and metabolism	0.81±0.03a	0.9±0.08b	0.67±0.02c
Secondary metabolism	0.29±0.01a	0.26±0.02b	0.27±0.006a,b
Dormancy and sporulation	0.108±0.007a	0.116±0.006b	0.1±0.01a
Detailed stress related genes			
Oxidative stress	1.2±0.02a	1.22±0.06a,b	1.24±0.04a,b
Osmotic stress	0.6±0.03a	0.55±0.05a	0.66±0.03b
Heat shock	0.27±0.01a	0.28±0.004a	0.3±0.009b
Detoxification	0.25±0.01a	0.25±0.02a	0.28±0.01b
Cold shock	0.033±0.003a,b	0.038±0.004a	0.033±0.003b
Acid stress	0.01±0.001a,b	0.013±0.003a	0.01±0.003a,b
Detailed virulence related genes			

Table 2. Characterization of the network interactions of microbial families on plastic samples at different CO_2 levels.

Table 2. Characterization of the network interactions of microbial families on plastic samples at different C

Network characteristics	Reference	Medium	High	
Nodes	362	391	327	
Edges	3431	3543	1038	
Average degree	9.478	9.061	3.174	
Network diameter	9	10	9	
Modularity	0.43	0.507	0.743	
Average clustering coefficient	0.233	0.257	0.184	
Average path length	2.71	2.659	2.348	
Most connected taxa	Rubrobacteraceae, Acidobacteriaceae, Comamonadaceae, Enterobacteriaceae	Pelobacteraceae, Nocardioidaceae, Beutenbergiaceae, Nitrospiraceae	Pseudomonadaceae, Pseudonocardiaceae, Nocardioidaceae, Streptomycetaceae	Th G

546

Table S1. Physiochemical water properties of the sampling locations at Shikine Island, Japa

Station	pH_T	Temp (°C)	Salinity (psu)	A_T (µmol kg^{-1})	pCO_2 (µatm)	DIC (µmol kg^{-1})	(µ
Reference	8.041	23.086	34.129	2281.9	409.965	2007.341	1
	0.067	0.603	0.741	6.8	73.383	38.944	
Medium	7.983	21.437	35.056	2282.93	493.011	2044.255	1
	0.119	1.273	0.125	6.57	158.004	53	
High	7.719	22.896	34.91	2271.84	970.706	2144.537	
	0.095	0.937	0.211	3.03	257.68	33.169	
Very High	7.529	22.072	34.723	2277.62	1803.047	2218.975	2
	0.234	1.212	0.742	20.5	1287.448	82.982	

547